ACADEMIC PRESS

Available online at www.sciencedirect.com

SCIENCE DIRECT®

Journal of Sound and Vibration 265 (2003) 417–435

JOURNAL OF SOUND AND VIBRATION

www.elsevier.com/locate/jsvi

Whirling motion of a shallow cable with viscous dampers

S.R.K. Nielsen[a,*], S. Krenk[b]

[a] *Department of Civil Engineering, Aalborg University, Sohngaardsholmsvej 57, DK-9000 Aalborg, Denmark*
[b] *Department of Mechanical Engineering, Technical University of Denmark, DK-2800 Kgs. Lyngby, Denmark*

Received 1 May 2002; accepted 23 July 2002

Abstract

The paper deals with the non-linear dynamic analysis of cables with a pair of viscous dampers close to one support. Such cables are characterized by a sag-to-chord-length ratio below 0.02, for which natural frequencies for the vertical and the horizontal vibrations are pair-wise close. Under resonance the non-linear coupling of pairs of modes may cause whirling harmonic motions around the chord line. Whirling motion may occur after bifurcation from single-mode response for harmonic loads in either vertical or horizontal direction. The non-linear features are included in the two coupled modes, while all other modes are treated as linear. The motion is discretized by expansion in terms of the damped complex eigenfunctions. The applied base functions fulfil the transition condition at the damper, leading to fast convergence of the expansion. It is demonstrated that the behaviour of the whirling motion is controlled primarily by the damper acting in the direction of the unloaded mode, whereas the magnitude of the damper in the loaded mode is less important. If the dampers in the vertical and horizontal direction are close to the optimal value of the corresponding taut cable case, substantial reduction of the vibration level of the whirling mode as well as the frequency interval of its occurrence is attained.
© 2002 Elsevier Science Ltd. All rights reserved.

1. Introduction

Cables used as structural elements in bridges and to support masts and towers are flexible and may hence be prone to excessive vibrations, either caused by wind or a combination of wind and rain, or by the motion of the supported structure, e.g. Ref. [1]. A common way to provide external damping is to mount a local viscous damper at a distance typically 2–4% of the span from one of the supports. The effect of the damper depends on the tuning: if the viscosity of the damper is too

*Corresponding author. Department of Civil Engineering, Aalborg University, Sohngaardsholmsvej 57, Aalborg 9000, Denmark.
E-mail address: soren.nielsen@civil.auc.dk (S.R.K. Nielsen).

0022-460X/03/$ - see front matter © 2002 Elsevier Science Ltd. All rights reserved.
doi:10.1016/S0022-460X(02)01455-4

high it will act as a support, and if the viscosity is too low it will fail to dissipate sufficient energy. Considering the case of a taut string and based on a semi-empirical approach, Kovacs [2] found that the maximum modal damping which could be provided by the damper was approximately half the relative distance of the damper from the support. An analytical solution to this problem was given by Krenk [3], who confirmed this result and obtained an accurate explicit asymptotic solution for the damping properties in terms of the complex wave number. The taut cable results are directly applicable to horizontal vibrations of cables with finite sag. The corresponding problem for vertical vibrations has recently been studied by Krenk and Nielsen [4], who derived explicit results for the modal damping ratios and for optimal tuning of the damper. The vertical modes of vibration separate into antisymmetric inextensional and symmetrical extensional modes. The former take place without dynamic extension of the cable, and hence have a low material dissipation of energy. However, the analysis showed that these modes may be effectively damped by a viscous damper. As for the taut cable problem the maximum damping ratio that can be obtained was approximately half the relative distance from the support. By contrast less effective damping may be obtained for the symmetrical extensional modes, because these modes develop regions of reduced vibration levels near the ends.

Forced response with coupled vertical and horizontal response has been analyzed in a number of studies based on two-degree-of-freedom (2 d.o.f.) models. Al-Noury and Ali [5] considered the harmonic response due to a uniformly distributed load with harmonic time variation, using a 2 d.o.f. Galerkin approach with sine functions used as shape functions, identical to the eigenmodes of the undamped taut cable. The same problem was dealt with by Rao and Iyengar [6], who used the undamped eigenmodes of the parabolic equilibrium approximation as a functional basis for the reduction to a 2 d.o.f. system. The use of the parabolic approximation is restricted to relatively small sag-to-chord-length ratios. An important dynamic load case for support cables as used in stay bridges and TV-towers is motion of the support points. The main effect on the non-linear response is the introduction of significant parametric terms, which may cause significant sub-, super- and combinatorial harmonic responses, Ref. [7].

The effect of forced support motion has been considered by Perkins [8], who obtained analytical solutions based on a first order perturbation analysis of a 2 d.o.f. model for coupled vertical and horizontal response using the undamped eigenmodes of the parabolic approximation to the static equilibrium suspension as a functional basis. The emphasis was on analysis of the 2:1 resonance phenomenon close to the so-called cross-over point of cables with relatively large sag-to-chord-length ratio, where an vertical harmonic resonance co-exists with a subharmonic resonance of the order 2 occurring in the horizontal modal co-ordinate. Lee and Perkins [9] extended the work to include second order perturbations and multiple internal resonances. Still, the focus was on 2:1 resonance, whereas the excitation was changed to a harmonic-varying uniformly distributed load acting in the static equilibrium plane. The same load was considered by Lee and Perkins [10] with emphasis on combined harmonic resonance in the vertical and horizontal modes. It was demonstrated that the stable response to the vertical excitation at a certain vibration level was a whirling motion involving a phase lag of $\pi/2$ between the linear mode shapes.

The present paper considers the non-linear harmonic response of a cable harmonically loaded in the static equilibrium state, and with discrete dampers located close to the lower support point acting orthogonal to the chord either in the vertical equilibrium plane or in the horizontal direction. The displacement components orthogonal to the chord are discretized by an expansion

in the damped eigenmodes, derived from the corresponding linear problem. In particular, harmonic resonance excitation in the lowest vertical and horizontal modes are considered. Because of the shallow cable assumptions the non-linear part of the response may be reduced to the analysis of a 2 d.o.f. system, involving a single vertical and a single horizontal mode. A first order perturbation solution to the non-linear modal co-ordinate equations of the 2-d.o.f. system is derived, and based on the derived model the capability of the damper acting in the horizontal direction to preventing coupled whirling motions is investigated.

2. Equations of non-linear cable vibrations

Fig. 1 shows a cable defined by the equilibrium state $y(x)$, the sag f and the chord length l, which is supported by two linear springs with the spring constants k_1 and k_2 acting along the chord. At the distance a from the support there is a pair of linear viscous dampers with the damper constant c_y and c_z acting in the vertical and horizontal directions, respectively. The total weight of the cable is W and the horizontal component of the equilibrium cable force is H. Within the shallow cable approximation the static curve of the cable is the parabola

$$y = 4f\left(1 - \frac{x}{l}\right)\frac{x}{l}, \tag{1}$$

where f and l are related to the chord force H as

$$Hf = \tfrac{1}{8}Wl. \tag{2}$$

The unit tangential vector at a certain point of the initial cable configuration with the co-ordinates $(x, y, 0)$ is given as

$$\mathbf{t}(x) = \frac{\mathrm{d}}{\mathrm{d}s}\begin{bmatrix} x \\ y \\ 0 \end{bmatrix}, \tag{3}$$

where $\mathrm{d}s$ denotes an infinitesimal cable element at the considered position. The material point of the initial cable configuration with the co-ordinates $(x, y, 0)$ undergoes the displacement vector $[u_x(x,t), u_y(x,t), u_z(x,t)]^T$ in the three co-ordinate directions. Then the unit tangential vector at the

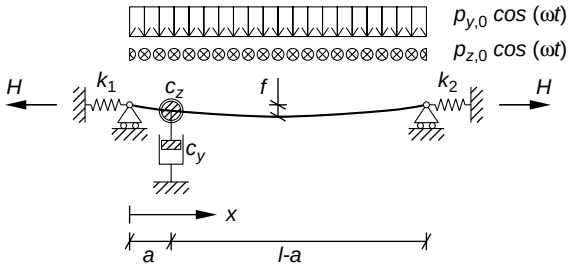

Fig. 1. Cable in equilibrium configuration.

considered point in the new configuration becomes

$$\mathbf{t}_1(x,t) = \frac{\partial}{\partial s_1}\begin{bmatrix} x+u_x \\ y+u_y \\ u_z \end{bmatrix} = \left(\mathbf{t}(x) + \frac{\partial}{\partial s}\begin{bmatrix} u_x \\ u_y \\ u_z \end{bmatrix}\right)\frac{\mathrm{d}s}{\mathrm{d}s_1}. \tag{4}$$

It follows from Eq. (4) that the initial and deformed length of the considered cable element are related as

$$\left(\frac{\mathrm{d}s_1}{\mathrm{d}s}\right)^2 = 1 + 2\left(\frac{\mathrm{d}x}{\mathrm{d}s}\frac{\partial u_x}{\partial s} + \frac{\mathrm{d}y}{\mathrm{d}s}\frac{\partial u_y}{\partial s}\right) + \left(\frac{\partial u_x}{\partial s}\right)^2 + \left(\frac{\partial u_y}{\partial s}\right)^2 + \left(\frac{\partial u_z}{\partial s}\right)^2. \tag{5}$$

The axial strain ε then follows from Eq. (5) as

$$\varepsilon = \frac{\mathrm{d}s_1 - \mathrm{d}s}{\mathrm{d}s} \simeq \frac{\mathrm{d}x}{\mathrm{d}s}\frac{\partial u_x}{\partial s} + \frac{\mathrm{d}y}{\mathrm{d}s}\frac{\partial u_y}{\partial s} + \frac{1}{2}\left(\frac{\partial u_y}{\partial s}\right)^2 + \frac{1}{2}\left(\frac{\partial u_z}{\partial s}\right)^2. \tag{6}$$

The term $\frac{1}{2}(\partial u_x/\partial s)^2$ is of magnitude ε^2, and has been omitted in comparison to the remaining terms on the right side of Eq. (5), which are all of the magnitude ε. To the same order of approximation

$$\frac{\mathrm{d}(x+u_x)}{\mathrm{d}s_1} = \left(1 + \frac{\partial u_x}{\partial x}\right)\frac{\mathrm{d}x}{\mathrm{d}s_1} \simeq \frac{\mathrm{d}x}{\mathrm{d}s}. \tag{7}$$

The increment of the component of the cable force in the x-direction must balance ΔH,

$$\Delta H = (F + \Delta F)\frac{\mathrm{d}(x+u_x)}{\mathrm{d}s_1} - F\frac{\mathrm{d}x}{\mathrm{d}s} \simeq \Delta F\frac{\mathrm{d}x}{\mathrm{d}s}, \tag{8}$$

where Eq. (7) has been used. The elasticity equation of the cable may then be written as

$$\Delta H\frac{\mathrm{d}s}{\mathrm{d}x} = EA\varepsilon. \tag{9}$$

Insertion of Eq. (6) and the introduction of x as independent parameter then provides

$$\Delta H\left(\frac{\mathrm{d}s}{\mathrm{d}x}\right)^3 = EA\left(\frac{\partial u_x}{\partial x} + \frac{\mathrm{d}y}{\mathrm{d}x}\frac{\partial u_y}{\partial x} + \frac{1}{2}\left(\frac{\partial u_y}{\partial x}\right)^2 + \frac{1}{2}\left(\frac{\partial u_z}{\partial x}\right)^2\right). \tag{10}$$

Due to the springs, the chord length will change by

$$\Delta l = -\Delta H\left(\frac{1}{k_1} + \frac{1}{k_2}\right). \tag{11}$$

Next, integration over l is performed in Eq. (10), and $\Delta l = u_x(l,t) - u_x(0,t)$ is eliminated by means of Eq. (11). After introduction of the non-dimensional abscissa $\xi = x/l$ the following relation is obtained:

$$\Delta H L_0 = \frac{EA}{l}\left(8f\int_0^l u_y\,dx + \frac{1}{2}\int_0^1 \left(\left(\frac{\partial u_y}{\partial \xi}\right)^2 + \left(\frac{\partial u_z}{\partial \xi}\right)^2\right)d\xi\right), \tag{12}$$

where

$$L_0 = L_e + EA\left(\frac{1}{k_1} + \frac{1}{k_2}\right) \tag{13}$$

and L_e denotes the so-called effective cable length,

$$L_e = \int_0^l \left(\frac{ds}{dx}\right)^3 dx \simeq \int_0^l \left(1 + \frac{3}{2}\left(\frac{dy}{dx}\right)^2\right) dx = l + 8\frac{f^2}{l}. \tag{14}$$

The approximation in the derivation of Eq. (14) introduces an error of the magnitude f^4/l^4.

The cable vibrations are caused by the distributed external loads $p_y(\xi, t)$ and $p_z(\xi, t)$ per unit length of the chord. Then the equations of motion for non-linear vibrations read

$$(H + \Delta H)\frac{\partial^2 u_y}{\partial \xi^2} - ml^2\frac{\partial^2 u_y}{\partial t^2} - c_y l\frac{\partial u_y}{\partial t}\delta(\xi - \alpha) - 8f\Delta H = -p_y(\xi, t)l^2, \tag{15}$$

$$(H + \Delta H)\frac{\partial^2 u_z}{\partial \xi^2} - ml^2\frac{\partial^2 u_z}{\partial t^2} - c_z l\frac{\partial u_z}{\partial t}\delta(\xi - \alpha) = -p_z(\xi, t)l^2, \tag{16}$$

where m denotes the mass per unit length of the cable, and the position of the damper is determined by the non-dimensional coordinate $\alpha = a/l$. Insertion of Eq. (12) into Eqs. (15) and (16) provides the equivalent equations

$$D_{1,r}(\mathbf{u}) + D_{2,r}(\mathbf{u}) + D_{3,r}(\mathbf{u}) = -p_r(\xi, t)l^2, \quad r = y, z, \tag{17}$$

where $\mathbf{u}^T(\xi, t) = [u_y(\xi, t), u_z(\xi, t)]$, and the index r specifies the co-ordinate direction. $D_{1,r}(\mathbf{u})$, $D_{2,r}(\mathbf{u})$ and $D_{3,r}(\mathbf{u})$ contains the linear, the quadratic and the cubic terms in the equation of motion in the co-ordinate direction r, respectively. These integro-differential operators are defined as follows:

$$D_{1,r}(\mathbf{u}) = H\left(\frac{\partial^2 u_r}{\partial \xi^2} - \lambda_r^2\int_0^1 u_r d\xi\right) - ml^2\frac{\partial^2 u_r}{\partial t^2} - c_r l\frac{\partial u_r}{\partial t}\delta(\xi - \alpha), \quad r = y, z, \tag{18}$$

$$D_{2,y}(\mathbf{u}) = 8f\frac{EA}{L_0 l}\left(\frac{\partial^2 u_y}{\partial \xi^2}\int_0^1 u_y d\xi - \frac{1}{2}\int_0^1 \left(\left(\frac{\partial u_y}{\partial \xi}\right)^2 + \left(\frac{\partial u_z}{\partial \xi}\right)^2\right) d\xi\right), \tag{19}$$

$$D_{2,z}(\mathbf{u}) = 8f\frac{EA}{L_0 l}\frac{\partial^2 u_z}{\partial \xi^2}\int_0^1 u_y d\xi, \tag{20}$$

$$D_{3,r}(\mathbf{u}) = \frac{1}{2}\frac{EA}{L_0 l}\frac{\partial^2 u_r}{\partial \xi^2}\int_0^1 \left(\left(\frac{\partial u_y}{\partial \xi}\right)^2 + \left(\frac{\partial u_z}{\partial \xi}\right)^2\right) d\xi, \quad r = y, z, \tag{21}$$

where λ_r^2 denotes the stiffness parameter defined by Irvine [11] as

$$\lambda_y^2 = 64\frac{EA}{H}\frac{f^2}{L_0 l}, \quad \lambda_z^2 = 0. \tag{22}$$

3. Damped linear eigenvibrations

Damped linear eigenvibrations are described by Eqs. (17) and (18),

$$H\left(\frac{\partial^2 u_r}{\partial \xi^2} - \lambda_r^2 \int_0^1 u_r d\xi\right) - ml^2 \frac{\partial^2 u_r}{\partial t^2} - c_r l \frac{\partial u_r}{\partial t}\,\delta(\xi-\alpha) = 0, \quad r = y, z. \tag{23}$$

Solutions to Eq. (23) are searched for in the form

$$u_r(\xi, t) = \tilde{u}_r(\xi) \mathrm{e}^{i\omega_r t}, \quad r = y, z, \tag{24}$$

where the amplitude functions $\tilde{u}_r(\xi)$ are solutions to the eigenvalue problems

$$\frac{\mathrm{d}^2 \tilde{u}_r}{\mathrm{d}\xi^2} - \lambda_r^2 \int_0^1 \tilde{u}_r d\xi + (\beta_r^2 - i\beta_r \eta_r \delta(\xi-\alpha))\tilde{u}_r = 0. \tag{25}$$

The solutions of Eq. (25) must fulfill the geometric boundary conditions $\tilde{u}_r(0) = \tilde{u}_r(1) = 0$. β_r and η_r denote a non-dimensional wave-number and non-dimensional damping constant given as

$$\beta_r = \omega_r l \sqrt{\frac{m}{H}}, \qquad \eta_r = \frac{c_r}{\sqrt{Hm}}, \quad r = y, z \tag{26, 27}$$

The discrete damper force is balanced by the transverse projection of the cable force before and after the support point of the damper. Formally, this effect is represented by the δ-function in Eq. (25). Alternatively, this may be formulated in terms of the transition conditions at $\xi = \alpha$:

$$\frac{\mathrm{d}\tilde{u}_r(\alpha^+)}{\mathrm{d}\xi} - \frac{\mathrm{d}\tilde{u}_r(\alpha^-)}{\mathrm{d}\xi} = \mathrm{i}\beta_r \eta_r \tilde{u}_r(\alpha). \tag{28}$$

It follows from Eqs. (25) and (28) that if $(i\omega_{r,j}, \tilde{u}_{r,j})$ denotes the jth eigensolution, then $(-i\omega_{r,j}^*, \tilde{u}_{r,j}^*)$ is another eigensolution, where $\omega_{r,j}^*$ is the complex conjugate of $\omega_{r,j}$. The solutions of Eq. (25), which fulfils the differential equation, the boundary conditions and the transition condition (28) are, [4],

$$\tilde{u}_r(\xi) = \begin{cases} \tilde{u}_{\alpha,r} \dfrac{\sin\beta_r\xi}{\sin\beta_r\alpha} + C_r \dfrac{(1-\cos\beta_r\xi)\sin\beta_r\alpha - (1-\cos\beta_r\alpha)\sin\beta_r\xi}{\beta_r^2 \sin\beta_r\alpha} \\ \tilde{u}_{\alpha,r} \dfrac{\sin\beta_r\xi'}{\sin\beta_r\alpha'} + C_r \dfrac{(1-\cos\beta_r\xi')\sin\beta_r\alpha' - (1-\cos\beta_r\alpha')\sin\beta_r\xi'}{\beta_r^2 \sin\beta_r\alpha'} \end{cases}, \tag{29}$$

where the upper formula applies for $\xi \leqslant \alpha$ and the lower for $\xi \geqslant \alpha$. The parameter C_r is defined as

$$C_r = \lambda_r^2 \int_0^1 \tilde{u}_r d\xi, \tag{30}$$

$\tilde{u}_{\alpha,r}$ denotes the undetermined amplitudes at $\xi = \alpha$, and $\xi' = 1-\xi$, $\alpha' = 1-\alpha$. For the horizontal vibrations $\lambda_z^2 = 0$, whereby $C_z = 0$. Hence, Eq. (29) reduces to the following simple taut cable form derived by Krenk [3]:

$$\tilde{u}_z(\xi) = \begin{cases} \tilde{u}_{\alpha,z} \dfrac{\sin\beta_z\xi}{\sin\beta_z\alpha}, & \xi \leqslant \alpha \\ \tilde{u}_{\alpha,z} \dfrac{\sin\beta_z\xi'}{\sin\beta_z\alpha'}, & \xi > \alpha \end{cases}. \tag{31}$$

The derivative of the eigenfunctions becomes

$$\frac{\mathrm{d}\tilde{u}_r}{\mathrm{d}\xi} = \begin{cases} \tilde{u}_{\alpha,r}\beta_r \dfrac{\cos\beta_r\xi}{\sin\beta_r\alpha} + C_r \dfrac{\sin\beta_r\xi\sin\beta_r\alpha - (1-\cos\beta_r\alpha)\cos\beta_r\xi}{\beta_r\sin\beta_r\alpha}, & \xi \leqslant \alpha \\ -\tilde{u}_{\alpha,r}\beta_r \dfrac{\cos\beta_r\xi'}{\sin\beta_r\alpha'} - C_r \dfrac{\sin\beta_r\xi'\sin\beta_r\alpha' - (1-\cos\beta_r\alpha')\cos\beta_r\xi'}{\beta_r\sin\beta_r\alpha'}, & \xi > \alpha \end{cases}. \tag{32}$$

Insertion of Eq. (29) into the transition condition (28) and into Eq. (30) provides the condition for the determination of the vertical eigenfrequencies

$$\begin{aligned} &\tan\left(\frac{\beta_y}{2}\right)\left(\tan\left(\frac{\beta_y}{2}\right) - \frac{\beta_y}{2} + \frac{4}{\lambda_y^2}\left(\frac{\beta_y}{2}\right)^3\right) \\ &\quad = -2i\eta_y \frac{\sin(\frac{\beta_y\alpha}{2})\sin(\frac{\beta_y\alpha'}{2})}{\cos(\frac{\beta_y}{2})}\left(\tan\left(\frac{\beta_y}{2}\right) - \frac{\cos(\frac{\beta_y\alpha}{2})\cos(\frac{\beta_y\alpha'}{2})}{\cos(\frac{\beta_y}{2})}\left(\frac{\beta_y}{2} - \frac{4}{\lambda_y^2}\left(\frac{\beta_y}{2}\right)^3\right)\right). \end{aligned} \tag{33}$$

Algorithms for the numerical solution of the complex eigenvalues β_y, including explicit asymptotic solutions valid for $\alpha \ll 1$, have been given in Ref. [4]. The corresponding frequency condition for the horizontal vibrations is derived by letting $\lambda_y^2 \to 0$ in Eq. (33), and changing the co-ordinate index from y into z.

$$\sin\beta_z = -i\eta_z \sin(\beta_z\alpha)\sin(\beta_z\alpha'). \tag{34}$$

Both vertical and horizontal eigenvibrations are separated into two groups for which the eigenmodes are approximately symmmetric and antisymmetric around $\xi = 0.5$, respectively. The index values $1, 3, 5, \ldots$ are used for the almost symmetric modes, and the indices $2, 4, 6, \ldots$ for the antisymmetric modes. Following Ref. [12] the orthogonality conditions for the linearized damped eigenmodes are most easily derived by writing Eq. (17) in the equivalent operator state vector formulation

$$\begin{bmatrix} K_r(\cdot) & 0 \\ 0 & ml^2 \end{bmatrix}\begin{bmatrix} u_r \\ \dot{u}_r \end{bmatrix} - \begin{bmatrix} c_r l\delta(\xi-\alpha) & ml^2 \\ ml^2 & 0 \end{bmatrix}\begin{bmatrix} \dot{u}_r \\ \ddot{u}_r \end{bmatrix} = \begin{bmatrix} f_r(\xi,t) \\ 0 \end{bmatrix}, \quad r = y, z, \tag{35}$$

where $\dot{u}_r = \partial u_r/\partial t$, and $K_r(\cdot)$ denotes the spatial operator

$$K_r(u_r) = H\left(\frac{\partial^2 u_r}{\partial\xi^2} - \lambda_r^2\int_0^1 u_r\,d\xi\right). \tag{36}$$

$f_r(\xi,t)$ includes both the external load and the non-linear terms of Eq. (17) as

$$f_r(\xi,t) = -p_r(\xi,t)l^2 - D_{2,r}(\mathbf{u}) - D_{3,r}(\mathbf{u}). \tag{37}$$

Obviously, $f_r(\xi,t) \equiv 0$ in case of linear eigenvibrations. From Eq. (24) follows that the jth linear eigenvibration solution to the homogeneous version of Eq. (35) has the form

$$\begin{bmatrix} u_r(\xi,t) \\ \dot{u}_r(\xi,t) \end{bmatrix} = \tilde{\mathbf{v}}_{r,j}(\xi)\mathrm{e}^{i\omega_{r,j}t}, \quad \tilde{\mathbf{v}}_{r,j}(\xi) = \begin{bmatrix} 1 \\ i\omega_{r,j} \end{bmatrix}\tilde{u}_{r,j}(\xi), \quad r = y, z. \tag{38}$$

Next, Eq. (38) is inserted into Eq. (35), followed by a scalar multiplication with $\tilde{\mathbf{v}}_{r,k}(\xi)$ and integration over the interval [0, 1]. This leads to the identity

$$\int_0^1 \tilde{\mathbf{v}}_{r,k}^T(\xi)\begin{bmatrix} K_r(\cdot) & 0 \\ 0 & ml^2 \end{bmatrix}\tilde{\mathbf{v}}_{r,j}(\xi)d\xi = i\omega_{r,j}\int_0^1 \tilde{\mathbf{v}}_{r,k}^T(\xi)\begin{bmatrix} c_r l\delta(\xi-\alpha) & ml^2 \\ ml^2 & 0 \end{bmatrix}\tilde{\mathbf{v}}_{r,j}(\xi)d\xi. \tag{39}$$

Since $K_r(\cdot)$ is a self-adjoint operator, Eq. (39) immediately provides the following orthogonality conditions:

$$\int_0^1 \tilde{\mathbf{v}}_{r,k}^T(\xi)\begin{bmatrix} K_r(\cdot) & 0 \\ 0 & ml^2 \end{bmatrix}\tilde{\mathbf{v}}_{r,j}(\xi)d\xi = -\omega_{r,j}M_{r,j}\delta_{jk}, \tag{40}$$

$$\int_0^1 \tilde{\mathbf{v}}_{r,k}^T(\xi)\begin{bmatrix} c_r l\delta(\xi-\alpha) & ml^2 \\ ml^2 & 0 \end{bmatrix}\tilde{\mathbf{v}}_{r,j}(\xi)d\xi = iM_{r,j}\delta_{jk}, \tag{41}$$

where $M_{r,j}$ denotes a modal mass defined as

$$\begin{aligned} M_{r,j} &= 2\omega_{r,j}ml^2\int_0^1 \tilde{u}_{r,j}^2(\xi)d\xi - ic_r l\tilde{u}_{r,j}^2(\alpha) \\ &= l\sqrt{Hm}\left(2\beta_{r,j}\int_0^1 \tilde{u}_{r,j}^2(\xi)d\xi - i\eta_r\tilde{u}_{r,j}^2(\alpha)\right). \end{aligned} \tag{42}$$

4. Forced non-linear vibrations

The solution of the non-linear forced vibration problem (35) is searched for in terms of the following expansion in the state vector eigenmodes for the vertical and horizontal motions, Ref. [12]

$$\begin{bmatrix} u_r(\xi,t) \\ \dot{u}_r(\xi,t) \end{bmatrix} = \sum_{j=1}^{\infty}(\tilde{\mathbf{v}}_{r,j}(\xi)q_{r,j}(t) + \tilde{\mathbf{v}}_{r,j}^*(\xi)q_{r,j}^*(t)). \tag{43}$$

Eq. (43) is inserted on the left sides of Eq. (35) and the resulting equation is multiplied scalarly with $\tilde{\mathbf{v}}_{r,k}(\xi)$, followed by an integration over the interval [0, 1]. Since $\tilde{\mathbf{v}}_{r,k}(\xi)$ is different from all the eigenmodes $\tilde{\mathbf{v}}_{r,j}^*(\xi)$, use of the orthogonality conditions (40) and (41) leads to the differential equation for the modal co-ordinate $q_{r,j}(t)$:

$$\dot{q}_{r,j} - i\omega_{r,j}q_{r,j} = f_{r,j}(t), \qquad f_{r,j}(t) = \frac{i}{M_{r,j}}\int_0^1 \tilde{u}_{r,j}(\xi)f_r(\xi,t)d\xi \tag{44, 45}$$

Insertion of Eq. (37) into Eq. (45) provides

$$f_{r,j}(t) = -\frac{i}{M_{r,j}}\int_0^1 \tilde{u}_{r,j}(\xi)(p_r(\xi,t)l^2 + D_{2,r}(\mathbf{u}) + D_{3,r}(\mathbf{u}))d\xi. \tag{46}$$

At first the linear response of Eq. (44) to a harmonic varying load per unit length acting in the y-direction with the circular frequency ω and the constant amplitude $p_{r,0}$ is investigated, i.e.,

$$p_r(\xi,t) = p_{r,0}\cos(\omega t), \tag{47}$$

where $p_{z,0} = 0$. Hence, the modal loading (46) may be written

$$f_{r,j}(t) = -i2F_{r,j}\cos(\omega t) = -iF_{r,j}(e^{i\omega t} + e^{-i\omega t}), \tag{48}$$

$$F_{r,j} = \frac{p_{r,0}l^2}{2M_{r,j}}\int_0^1 \tilde{u}_{r,j}(\xi)d\xi. \tag{49}$$

Then, the stationary linear harmonic response to Eq. (44) becomes

$$q_{r,j}(t) = F_{r,j}\left(\frac{e^{i\omega t}}{\omega_{r,j} - \omega} + \frac{e^{-i\omega t}}{\omega_{r,j} + \omega}\right). \tag{50}$$

Since the damping of the cable is presumed to be small, the denominator in the first term of the right side of (50) becomes large as $\omega \to |\omega_{r,j}|$, whereas the second term remains small. Hence, under resonance amplification the modal coordinate $q_{r,j}(t)$ may be written approximately as

$$q_{r,j}(t) \simeq \frac{e^{i\omega t}}{\omega_{r,j} - \omega}F_{r,j}. \tag{51}$$

Formally, Eq. (51) provides the stationary harmonic response, if the real time variation $\cos(\omega t)$ in Eq. (48) is replaced with the complex harmonic excitation $\frac{1}{2}e^{i\omega t}$. This approximation, which is only valid under strong resonance, will be used below.

The main effect of including the non-linear terms through the differential operators $D_{2,r}(\xi, t)$ and $D_{3,r}(\xi, t)$ in Eqs. (37), (45) is, in addition to generating some less important harmonics (including a static component), to cause qualitative and quantitative corrections to the described linear harmonic response. Hence, the next step is to calculate these corrections, which are only of importance under resonance. This suggests that a truncated modal expansion only involving the first vertical and horizontal modal co-ordinate $q_{y,1}$ and $q_{z,1}$ need to be considered at the evaluation of the non-linear terms entering through the modal load, whereas all other modal co-ordinates may be evaluated from the linear analysis presented above. For ease of notation the index $j = 1$ for the non-linear modes are omitted in the following derivations, so $q_r(t) = q_{r,1}$, etc.

The harmonic component of the modal co-ordinates may be written as

$$q_r(t) = Q_r e^{i\Phi_r}, \quad \Phi_r = \omega t + \Psi_r. \tag{52}$$

Q_r denotes the amplitude of the modal co-ordinate, and Ψ_r is the phase relative to excitation (47). Hence, the introduced approximations imply that the displacement field attains the form, cf., (38) and (43),

$$u_r(\xi, t) \simeq 2Q_r \mathrm{Re}[\tilde{u}_r(\xi)e^{i\Phi_r}] = 2Q_r(A_r(\xi)\cos\Phi_r - B_r(\xi)\sin\Phi_r), \tag{53}$$

where $A_r(\xi) = \mathrm{Re}[\tilde{u}_r(\xi)]$ and $B_r(\xi) = \mathrm{Im}[\tilde{u}_r(\xi)]$.

In the following it is assumed that the eigenmodes are normalized to unity at the midpoint, i.e., $\tilde{u}_r(0.5) = 1$. Further, if the damping of the cable is low, as is the case for $\alpha < 0.02$, $B_r(\xi)$ amounts to a few percent of $A_r(\xi)$ as seen for the example shown in Fig. 2. Hence, the term $B_r(\xi)\sin\Phi_r$ may be ignored in Eq. (53), so

$$u_r(\xi, t) \simeq 2Q_r A_r(\xi)\cos\Phi_r(t). \tag{54}$$

Because of the applied normalization $2Q_r\cos\Phi_r(t)$ may be interpreted as the displacement of the midpoint of the cable in the co-ordinate direction r. Upon insertion of the harmonic response (54)

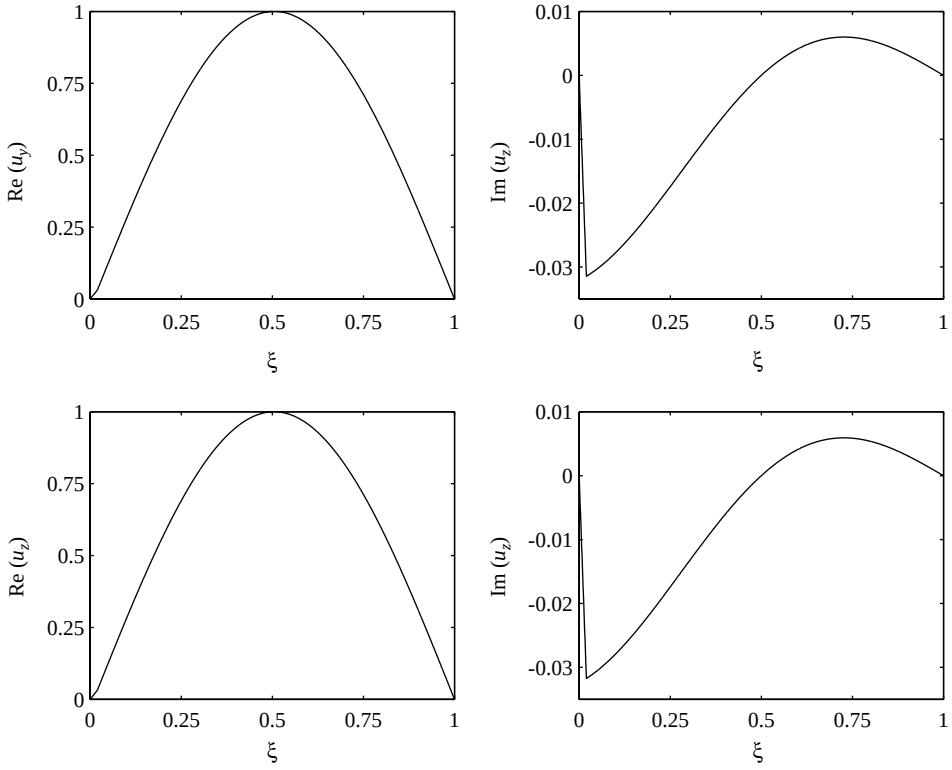

Fig. 2. Real and imaginary parts of normalized mode shapes. $\alpha = 0.02$, $c_{y0} = c_{z0} = 1.0$.

into Eqs. (19)–(21) the quadratic and cubic operators $D_{2,r}(\xi, t)$ and $D_{3,r}(\xi, t)$ become periodic in time. Insertion into $D_{2,r}(\xi, t)$ provides harmonic terms of the zeroth and second order. Hence, the quadratic non-linear operator does not affect the non-linear harmonic response at the considered first-order perturbation level. This is a consequence of considering only external loads on the cable. Alternatively, if support point motions have been considered, parametric terms are introduced in the equations of motion due to the elongations of the chord, which leads to a substantial harmonics in the vertical component of the quadratic non-linear operator. The cubic operator provides, cf., (21),

$$D_{3,r}(\xi,t) \simeq \frac{8}{2}\frac{EA}{L_0 l}\frac{\mathrm{d}^2 A_r}{\mathrm{d}\xi^2}\cos\Phi_r Q_r \int_0^1 \left(Q_y^2 \left(\frac{\mathrm{d}A_y}{\mathrm{d}\xi}\cos\Phi_y\right)^2 + Q_z^2 \left(\frac{\mathrm{d}A_z}{\mathrm{d}\xi}\cos\Phi_z\right)^2 \right) d\xi$$

$$= \frac{EA}{L_0 l}\frac{\mathrm{d}^2 A_r}{\mathrm{d}\xi^2} Q_r \Bigg((2\cos\Phi_r + \cos(\Phi_r + 2\Psi_y - 2\Psi_r)) Q_y^2 \int_0^1 \left(\frac{A_y}{d\xi}\right)^2 d\xi$$

$$+ (2\cos\Phi_r + \cos(\Phi_r + 2\Psi_z - 2\Psi_r)) Q_z^2 \int_0^1 \left(\frac{A_z}{d\xi}\right)^2 d\xi \Bigg) + \cdots$$

$$= \frac{1}{2}\frac{EA}{L_0 l}\frac{\mathrm{d}^2 A_r}{\mathrm{d}\xi^2} Q_r \left(Q_y^2 (2 + \mathrm{e}^{\mathrm{i}2(\Psi_y - \Psi_r)}) \int_0^1 \left(\frac{A_y}{\mathrm{d}\xi}\right)^2 \mathrm{d}\xi \right.$$

$$\left. + Q_z^2 (2 + \mathrm{e}^{i2(\Psi_z - \Psi_r)}) \int_0^1 \left(\frac{A_z}{d\xi}\right)^2 d\xi \right) \mathrm{e}^{i\Psi_r} \mathrm{e}^{i\omega t} + \cdots \tag{55}$$

where the dots indicate unspecified harmonics of the third order. Further, cosine terms of the type $\cos(\omega t + \varphi)$ have been replaced by the equivalent complex harmonics $\frac{1}{2}\mathrm{e}^{\mathrm{i}(\omega t + \varphi)}$ in the last statement, cf., Eq. (51). In Eq. (55) the approximation $A_z(\xi) \simeq \sin(\pi\xi)$ may always be used for further reduction of the expression. The corresponding approximation for $A_y(\xi)$ is not applicable unless the stiffness parameter λ_y^2 is well below say 20 due to the occurrence of reverse motion near the supports, see Ref. [4]. Insertion of Eq. (55) into Eqs. (44), (45), and retaining only the harmonic terms of first order, provides the following algebraic equations for the determination of the amplitudes Q_r and phases Ψ_r of the harmonic modal response

$$(\omega_r - \omega + a_{ry}(2 + \mathrm{e}^{\mathrm{i}2(\Psi_y - \Psi_r)})Q_y^2 + a_{rz}(2 + \mathrm{e}^{\mathrm{i}2(\Psi_z - \Psi_r)})Q_z^2)Q_r \mathrm{e}^{\mathrm{i}\Psi_r} = F_r. \tag{56}$$

where F_r is given by Eq. (49), and the constants a_{rs} are defined as

$$a_{rs} = \frac{1}{2M_r}\frac{EA}{L_0 l}\int_0^1 \frac{\mathrm{d}\tilde{u}_r}{\mathrm{d}\xi}\frac{\mathrm{d}A_r}{\mathrm{d}\xi} d\xi \int_0^1 \left(\frac{\mathrm{d}A_s}{\mathrm{d}\xi}\right)^2 d\xi, \quad r, s = y, z. \tag{57}$$

Although omitted here analytical expressions for a_{rs}, M_r and F_r may be evaluated based on Eqs. (31) and (32). It follows from Eq. (57) that the fractions a_{yy}/a_{yz} and a_{zz}/a_{zy} are both real, and that $a_{yy}a_{zz}/(a_{yz}a_{zy}) = 1$.

5. Non-linear harmonic response analysis

The set of equations (56) is seen to be symmetric in the directions y and z, where the only difference is in the precise definition of the coefficients a_{rs}. Assuming that the harmonic excitation is only acting in one of the two directions, the analysis may then be performed for this setup of the load. Then, the corresponding results for the load acting in the other direction can be derived by a change of indices from the obtained solution. Hence, by considering the case of loading in the vertical plane, $F_z = 0$, and Eq. (56) may be written in terms of the equivalent equations

$$(\omega_y - \omega + 3a_{yy}Q_y^2 + (2 + \mathrm{e}^{i2\Psi})a_{yz}Q_z^2)Q_y \mathrm{e}^{i\Psi_y} = F_y, \tag{58}$$

$$(\omega_z - \omega + 3a_{zz}Q_z^2 + (2 + \mathrm{e}^{-i2\Psi})a_{zy}Q_y^2)Q_z \mathrm{e}^{i\Psi_z} = 0, \tag{59}$$

where $\Psi = \Psi_z - \Psi_y$ denotes the phase difference between the modal co-ordinates.

The second equation is homogeneous and can be satisfied in two ways: either Q_z vanishes identically, or the large parentheses are identically zero. The first case corresponds to motion in the vertical plane—the plane of the load—while the second case leads to coupling between the motion in the y- and z-planes, so-called whirling motion.

5.1. Vertical motion

In this case $Q_z = 0$ and the remaining equation (58) can be rewritten as an expression for the phase angle Ψ_y in terms of the frequency ω and the response amplitude Q_y,

$$e^{-i\Psi_y} = (\omega_y - \omega + 3a_{yy}Q_y^2)\frac{Q_y}{F_y}. \tag{60}$$

An equation for the amplitude Q_y is obtained by multiplication of both sides of Eq. (60) with their complex conjugates. This leads to the following cubic equation in Q_y^2,

$$(|\Omega_y|^2 + 6\mathrm{Re}[\Omega_y]Q_y^2 + 9Q_y^4)Q_y^2 = \left|\frac{F_y}{a_{yy}}\right|^2, \tag{61}$$

where the normalized difference of the frequency from the natural frequency of the vertical motion is conveniently introduced as

$$\Omega_y = \frac{\omega_y - \omega}{a_{yy}}. \tag{62}$$

Eq. (61) may have one, two or three positive real solutions for Q_y^2, which all determines a possible harmonic motion. However, in the case of three solutions only the motions with the largest and the smallest amplitudes are stable according to a Lyapunov first order perturbation instability criterium. The associated phase Ψ_y is next determined as the negative argument of the right side of Eq. (60) with the relevant solution for Q_y inserted. Bearing in mind that $2Q_y$ denotes the amplitude of the harmonic response at the mid-point, Eq. (61) may be considered as the amplitude relation for a standard Duffing oscillator with a hardening non-linear parameter ε determined from $\frac{3}{4}\varepsilon = \frac{3}{8}|a_{yy}|$.

5.2. Whirling motion

The whirling motion is determined from the solution corresponding to vanishing of the first factor in Eq. (59),

$$\omega_z - \omega + 3a_{zz}Q_z^2 + (2 + e^{-i2\Psi})a_{zy}Q_y^2 = 0. \tag{63}$$

The connection between the motion in the y- and the z-plane is determined by isolating the phase angle Ψ in Eq. (63). This implies writing the equation in the form:

$$\frac{\omega_z - \omega}{a_{zy}} + \left(2Q_y^2 + 3\frac{a_{zz}}{a_{zy}}Q_z^2\right) = -Q_y^2 e^{-i2\Psi}. \tag{64}$$

Comparison with Eq. (62) the notation is introduced for the normalized difference of the frequency from the natural frequency in the horizontal direction as

$$\Omega_z = \frac{\omega_z - \omega}{a_{zy}} \tag{65}$$

for the normalized difference between the frequency ω and the natural frequency ω_z for the horizontal motion.

It is noted that the ratio a_{zz}/a_{zy} is real, and thus the parentheses are real. A simple relation for the phase angle in terms of the normalized frequency can therefore be obtained by subtracting the

conjugated equation from Eq. (64), whereby

$$\sin(2\Psi) = \frac{\mathrm{Im}[\Omega_z]}{Q_y^2}. \tag{66}$$

Another relation, for the amplitude ratio Q_z/Qy, is obtained by multiplication of both sides of Eq. (64) with their complex conjugate. When it is noted that the parentheses are real, this gives the relation

$$\left(2Q_y^2 + 3\frac{a_{zz}}{a_{zy}}Q_z^2\right)^2 + 2\mathrm{Re}[\Omega_z]\left(2Q_y^2 + 3\frac{a_{zz}}{a_{zy}}Q_z^2\right) + |\Omega_z|^2 = Q_y^4. \tag{67}$$

This is a quadratic equation in Q_z^2, whereby the solution takes the form

$$\frac{a_{zz}}{a_{zy}}Q_z^2 = -\frac{1}{3}\left(2Q_y^2 + \mathrm{Re}[\Omega_z] \pm \sqrt{Q_y^4 - \mathrm{Im}[\Omega_z]^2}\right). \tag{68}$$

This relation determines the amplitude Q_z in terms of Q_y and the normalized frequency Ω_z.

If the cable is undamped in the horizontal direction (i.e., $c_z = 0$), then $\mathrm{Im}[\Omega_z] = 0$ and the phase difference becomes exactly $\Psi = \pm\pi/2$, or $\Psi = 0, \pi$. In case of whirling motions the semi-axes of the trajectory become parallel to the modal co-ordinate axes. Since, $|\mathrm{Im}[\Omega_z]| \ll Y$, it follows from Eq. (66) that solutions in Eq. (68) with "+" and "−" signs in front of the square root determines phase motions and whirling motions, respectively. All phase motions turn out to be unstable, and will not be analyzed further.

In addition to two relations (66) and (68) equations are required for the phase angle Ψ_y and the amplitudes Q_y. First, a relation is obtained for the phase angle Ψ_y by multiplication of Eq. (58) with a_{yz}/a_{yy},

$$\frac{\omega_y - \omega}{a_{yy}} + \left(2\frac{a_{zz}}{a_{zy}}Q_z^2 + 3Q_y^2\right) + \left(\frac{a_{zz}}{a_{zy}}Q_z^2\right)\mathrm{e}^{i2\Psi} = \frac{\mathrm{e}^{-i\Psi_y}}{a_{yy}}\frac{F_y}{Q_y}, \tag{69}$$

where it has been used that $a_{yz}/a_{yy} = a_{zz}/a_{zy}$. The phase angle Ψ can be eliminated from Eq. (69) by multiplication with Q_y^2 and substitution of the conjugate of Eq. (64)

$$\Omega_y Q_y^2 - \Omega_z^*\left(\frac{a_{zz}}{a_{zy}}Q_z^2\right) + 3Q_y^4 - 3\left(\frac{a_{zz}}{a_{zy}}Q_z^2\right)^2 = \mathrm{e}^{-i\Psi_y}\frac{F_y}{a_{yy}}Q_y. \tag{70}$$

Multiplication of both sides of this equation with their complex conjugate leads to the equation

$$\left[3Q_y^4 - 3\left(\frac{a_{zz}}{a_{zy}}Q_z^2\right)^2\right]^2 + 2\left[\mathrm{Re}[\Omega_y]Q_y^2 - \mathrm{Re}[\Omega_z]\left(\frac{a_{zz}}{a_{zy}}Q_z^2\right)\right]\left[3Q_y^4 - 3\left(\frac{a_{zz}}{a_{zy}}Q_z^2\right)^2\right] + \left|\Omega_y Q_y^2 - \Omega_z^*\left(\frac{a_{zz}}{a_{zy}}Q_z^2\right)\right|^2 = \frac{F_y^2}{|a_{yy}|^2}Q_y^2. \tag{71}$$

Collecting terms leads to

$$9Q_y^8 + 6\mathrm{Re}[\Omega_y]Q_y^6 + |\Omega_y^2|Q_y^2 - [18Q_y^4 + 6\mathrm{Re}[\Omega_y]Q_y^2]\left(\frac{a_{zz}}{a_{zy}}Q_z^2\right)^2$$
$$- [6\mathrm{Re}[\Omega_z]Q_y^4 + 2\mathrm{Re}[\Omega_y\Omega_z]Q_y^2]\left(\frac{a_{zz}}{a_{zy}}Q_z^2\right)$$
$$+ \left\{9\left(\frac{a_{zz}}{a_{zy}}Q_z^2\right)^2 + 6\mathrm{Re}[\Omega_z]\left(\frac{a_{zz}}{a_{zy}}Q_z^2\right) + |\Omega_z|^2\right\}\left(\frac{a_{zz}}{a_{zy}}Q_z^2\right)^2 = \frac{F_y^2}{|a_{yy}|^2}Q_y^2. \tag{72}$$

The terms in the braces are evaluated from Eq. (67), whereby Q_y^2 appears as a factor to all terms of the equation. After removing the common factor Q_y^2 the equation is

$$9Q_y^6 + 6\mathrm{Re}[\Omega_y]Q_y^4 + |\Omega_y^2|Q_y^2 - [6\mathrm{Re}[\Omega_z]Q_y^2 + 2\mathrm{Re}[\Omega_y\Omega_z]]\left(\frac{a_{zz}}{a_{zy}}Q_z^2\right)$$
$$- \left[21Q_y^2 + 6\mathrm{Re}[\Omega_y] + 4\mathrm{Re}[\Omega_z]\right]\left(\frac{a_{zz}}{a_{zy}}Q_z^2\right)^2 - 12\left(\frac{a_{zz}}{a_{zy}}Q_z^2\right)^3 = \frac{F_y^2}{|a_{yy}|^2}. \tag{73}$$

In this equation Q_z^2 can be eliminated by use of solution (68). The solution with the minus sign is used, as this solution represents the whirling motion as already mentioned. The result is an equation of the form

$$(A_1 + A_2Q_y^2 + 32Q_y^4)\sqrt{Q_y^4 - \mathrm{Im}[\Omega_z]^2} = A_0 + A_2Q_y^2 - A_3Q_y^4 - 32Q_y^6, \tag{74}$$

with the coefficients

$$A_0 = 9F_y^2/|a_{yy}|^2 - 6\mathrm{Re}[\Omega_y\Omega_z^*]\mathrm{Re}[\Omega_z] - (6\mathrm{Re}[\Omega_y] - 8\mathrm{Re}[\Omega_z])\,\mathrm{Im}[\Omega_z]^2,$$

$$A_1 = 6\mathrm{Re}[\Omega_y\Omega_z^*] - 4\mathrm{Re}[\Omega_z]^2 + 4\mathrm{Im}[\Omega_z]^2,$$

$$A_2 = -9|\Omega_y|^2 + 12\mathrm{Re}[\Omega_y\Omega_z^*] - 5\mathrm{Re}[\Omega_z]^2 + 3\mathrm{Im}[\Omega_z]^2, \qquad A_3 = 16\mathrm{Re}[\Omega_z]. \tag{75}$$

Finally, Eq. (74) can be reduced to a quartic equation in Q_y^2 by squaring both sides.

$$B_0 + B_1Q_y^2 + B_2Q_y^4 + B_3Q_y^6 - B_4Q_y^8 = 0. \tag{76}$$

The coefficients of this equation are combinations of the coefficients (75),

$$B_0 = A_0^2 + A_1^2\,\mathrm{Im}[\Omega_z]^2, \qquad B_1 = 2A_0A_2 + 2A_1A_3\mathrm{Im}[\Omega_z]^2,$$

$$B_2 = -A_1^2 + A_2^2 - 2A_0A_3 + (A_3^2 + 64A_1)\,\mathrm{Im}[\Omega_z]^2,$$

$$B_3 = -2(A_1 + A_2)A_3 - 64A_0 + 64A_3\,\mathrm{Im}[\Omega_z]^2,$$

$$B_4 = -64(A_1 + A_2) + 1024\mathrm{Im}[\Omega_z]^2. \tag{77}$$

The quartic equation (76) may have either four real solutions, two real solution and two complex-conjugated solutions or two pairs of complex-conjugated solutions. Negative real and

complex solutions contradict the basic assumption of real amplitudes and must be discarded as false. For any positive real solution Q_y^2, the corresponding solution for Q_z^2 and $\Psi = \Psi_z - \Psi_y$ follows from Eqs. (68) and (66), using the negative sign in front of the square root. Finally, Ψ_y is obtained from Eq. (70).

Further, in case that more than one whirling solution exists, only the one, which is generated by bifurcation from the vertical solution turns out to be Lyapunov stable.

6. Numerical example

The data of the considered cable refers to the longest stay in the cable-stayed bridge across the Øresund between Denmark and Sweden. The supports are assumed fixed, corresponding to $k_1 = k_2 = \infty$. The stiffness of the cable is $EA = 2.17 \times 10^9$ N, and the equilibrium force $H = 5.5 \times 10^6$ N. The chord length is 260 m, and the cable mass is $m = 81.05$ kg/m, corresponding to a total weight of $W = 2.038 \times 10^5$ N. The intensity of the oscillating load is selected as $p_{y,0} = p_{z,0} = 0.15\ W/l$.

The damping constants are specified as $c_y = c_{y0}c_{\text{opt}}$ and $c_z = c_{z0}c_{\text{opt}}$, where $c_{\text{opt}} = \sqrt{Hm}/(\pi\alpha)$ denotes the optimal damping constant for a taut cable, Ref. [3]. In case the damper constant is smaller than the optimal value less energy is dissipated due to the reduced viscosity. A larger damper constant will also lead to reduced energy dissipation, because the damper in this case tends to block the displacement of the support point. The intention of the following examples is to investigate the effect of the factors c_{y0} and c_{z0} on the whirling response.

Fig. 2 shows the real and imaginary part of the first vertical and horizontal modes of the linearized problem with the normalization $\tilde{u}_r(0.5) = 1$, using the parameter values $\alpha = 0.02$ and $c_{y0} = c_{z0} = 1.0$. As seen the real parts are almost smooth at the attachment of the damper, and the imaginary part is everywhere very small.

Figs. 3 and 4 show the possible harmonic response in terms of the modal co-ordinates $q_y(t)$ and $q_z(t)$ as functions of the non-dimensional excitation frequency $\Omega = \omega/|\omega_z|$, for vertical and horizontal loading, respectively. Both figures correspond to vibrations of the cable without dampers, i.e., $c_{y,0} = c_{z,0} = 0$. Solid lines denote branches with stable solutions according to a first order Lyapunov stability analysis, whereas branches with dashed signature denote unstable solutions. As stated in relation to Eq. (54) $2Q_y$ and $2Q_z$ denote the amplitudes of the midpoint of the cable. In all shown figures the phase difference Ψ has been normalized with respect to $\pi/2$. Hence, Ψ attains exactly the value $\pi/2$ in Figs. 3 and 4 for both stable and unstable branches as a consequence of the cable being undamped in the vertical direction. The in-plane harmonic response remains stable up to a critical level as indicated by the point A in the figures, where a transition to the stable whirling mode takes place. The amplitude response curves in the two figures are much alike, although transition to whirling motion takes place at a somewhat higher level in the horizontal load case in Fig. 4.

Figs. 5–7 display the modal amplitudes in the vertical load case, when the vertical damper is kept at the optimal taut cable value, while the horizontal damper is varied through the values 0.05, 1.0 and 20.0 times the optimal taut cable value.

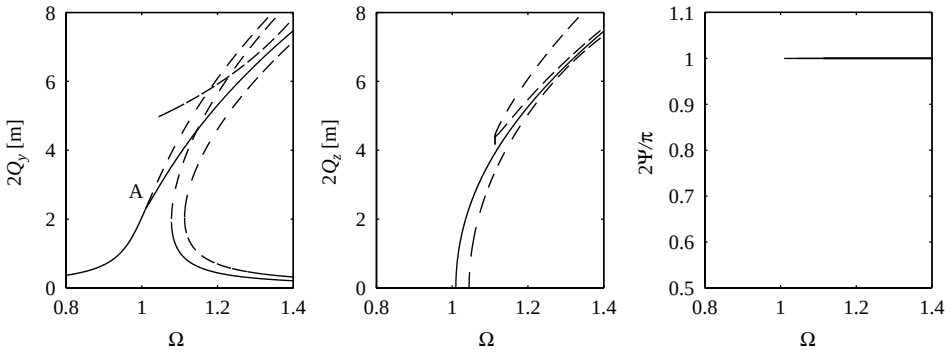

Fig. 3. Harmonic amplitude response, vertical loading. $p_{y,0} = 0.15W/l$, $\alpha = 0.02$, $c_{y0} = 0.0$, $c_{z0} = 0.0$: ——, stable solutions; - - - -, unstable solutions.

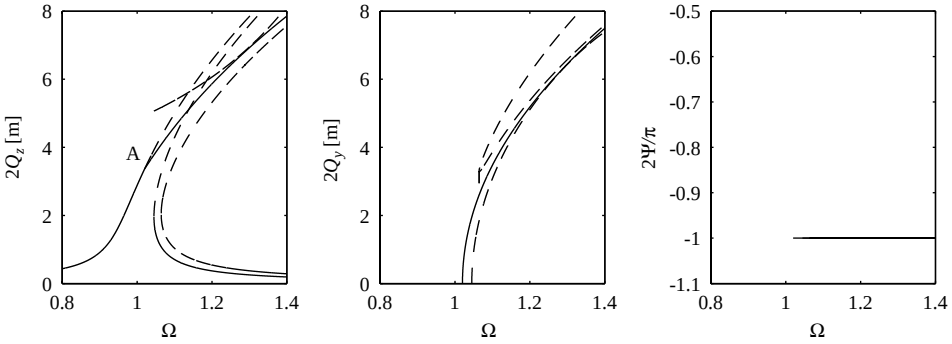

Fig. 4. Harmonic amplitude response, horizontal loading. $p_{z,0} = 0.15W/l$, $\alpha = 0.02$, $c_{y0} = 0.0$, $c_{z0} = 0.0$: ——, stable solutions; - - - -, unstable solutions.

The modal damping ratio ζ_r of a complex mode may be defined in terms of the complex damped frequency ω_r of the mode by the relationship

$$\omega_r = |\omega_r|\left(\sqrt{1-\zeta_r^2} + i\zeta_r\right). \tag{78}$$

For the small damping $c_{z0} = 0.05$ the taut cable frequency is $|\omega_z| = 3.1478/\text{s}$ and the damping ratio is $\zeta_z = 9.964 \times 10^{-4}$, while for the large damping $c_{z0} = 20.0$ the taut cable frequency is $|\omega_z| = 3.2117/\text{s}$ while the damping ratio is $\zeta_z = 9.977 \times 10^{-4}$. Thus, the damping ratio of the horizontal oscillations are very similar for Figs. 5 and 7. It is seen that the stable branch of the whirling motion is also much alike in the two cases. By contrast, the unstable branches are sensitive to the magnitude of circular eigenfrequency, which is increased in the case shown in Fig. 7, because of the shortening of the cable length, caused by the locking of the cable due to the large damping constant.

For the case shown in Fig. 6, where the damper in the horizontal direction is at the optimal taut cable value, a qualitatively different pattern is observed. Firstly, whirling motions are confined to a much smaller frequency interval following the bifurcation point. Secondly, the maximum

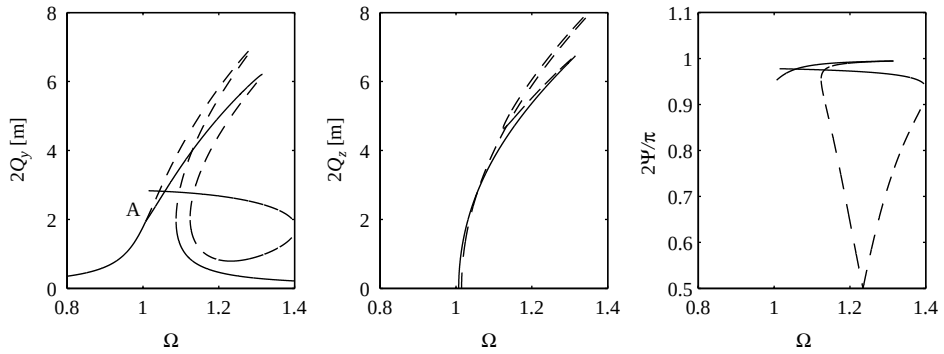

Fig. 5. Harmonic amplitude response, vertical loading. $p_{y,0} = 0.15W/l$, $\alpha = 0.02$, $c_{y0} = 1.0$, $c_{z0} = 0.05$: ——, stable solutions; - - - -, unstable solutions.

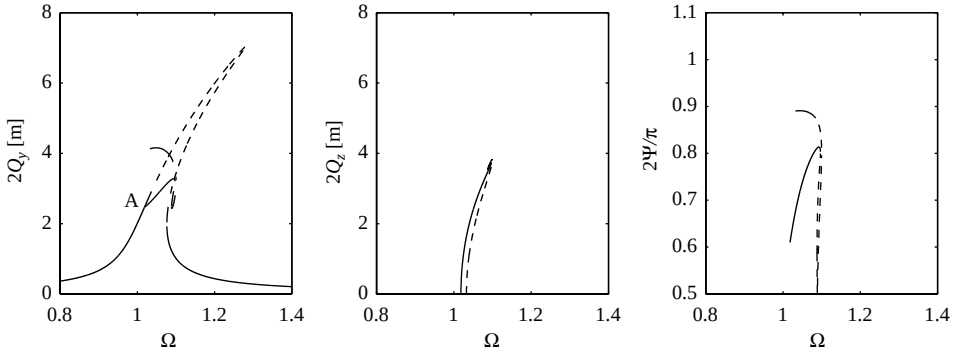

Fig. 6. Harmonic amplitude response, vertical loading. $p_{y,0} = 0.15W/l$, $\alpha = 0.02$, $c_{y0} = 1.0$, $c_{z0} = 0.05$: ——, stable solutions; - - - -, unstable solutions.

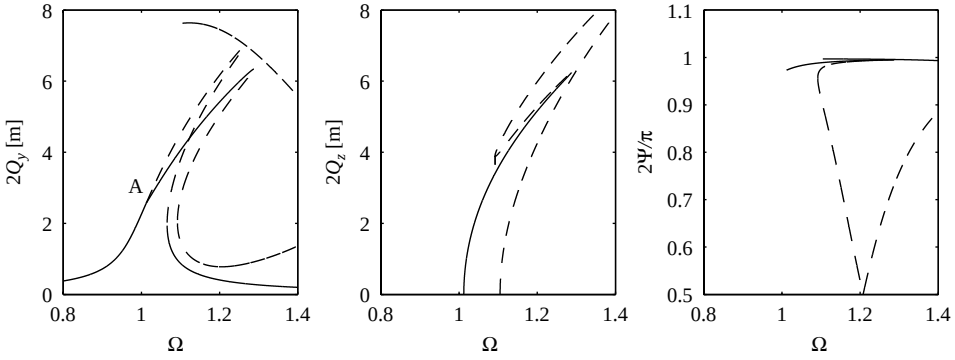

Fig. 7. Harmonic amplitude response, vertical loading. $p_{y,0} = 0.15W/l$, $\alpha = 0.02$, $c_{y0} = 1.0$, $c_{z0} = 20.0$: ——, stable solutions; - - - -, unstable solutions.

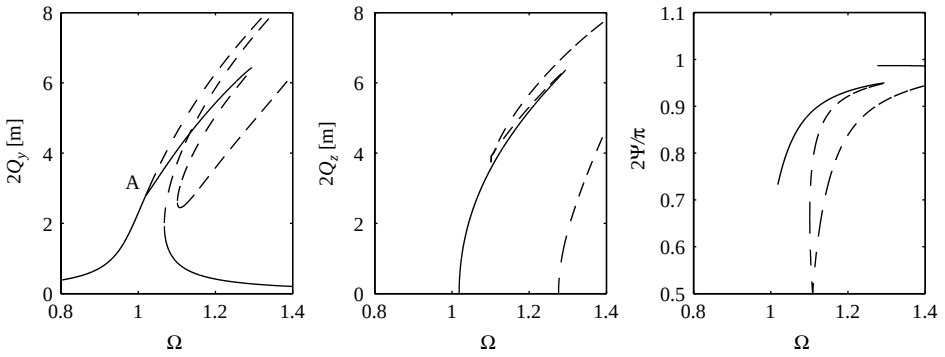

Fig. 8. Harmonic amplitude response, vertical loading. $p_{y,0} = 0.15W/l$, $\alpha = 0.02$, $c_{y0} = 1.0$, $c_{z0} = 20.0$: ——, stable solutions; - - - -, unstable solutions.

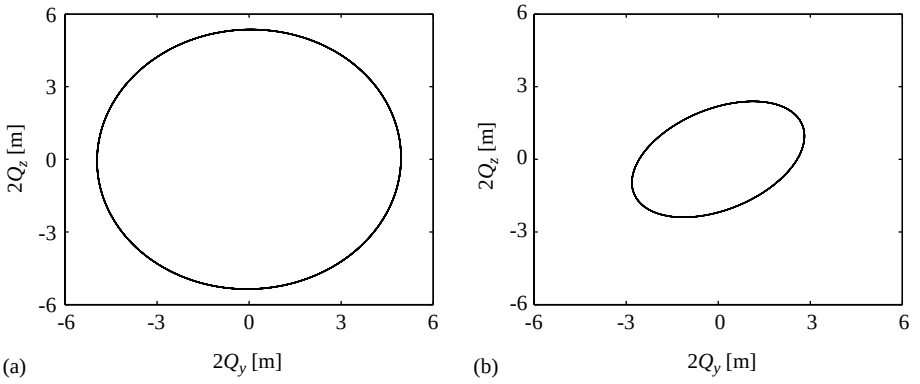

Fig. 9. Trajectories of cable midpoint in whirling mode of motion. $p_{y,0} = 0.15W/l$, $\alpha = 0.02$. (a) $c_{y0} = 1.0$, $c_{z0} = 0.05$, $\Omega = 1.2$; (b) $c_{y0} = 1.0$, $c_{z0} = 1.0$, $\Omega = 1.05$.

vibration amplitudes encountered during whirling motions are significantly smaller than those displayed in Figs. 5 and 7. It is also interesting to note that the transition to whirling motion reduces the maximum vibration amplitudes compared to the maximum amplitude of the vertical mode in single-mode response, presuming this to be stable beyond the bifurcation point.

The previous observations suggest that qualitative behaviour of whirling motion is strongly influenced by the damping constant in the unloaded mode, i.e., c_z in Figs. 5–7. Fig. 8 shows a case where the vertical mode has very low damping, resulting in excessive single-mode response. The damper in the horizontal direction is the same as for the case in Fig. 6. The results of Figs. 6 and 8, corresponding to interchange of the dampers, show similar magnitude of the whirling motion but a slight difference in the phase angle.

In Fig. 9 is shown the trajectory of the midpoint of the cable under whirling motion for optimal damping of the loaded vertical mode, while the horizontal damping is low (Fig. 9(a)) or optimal (Fig. 9(b)) corresponding to Figs. 5 and 6, respectively. It is seen that the optimal damping in both directions the semi-axes of the elliptic trajectory is slightly tilted, and the size of the ellipse is considerable smaller.

7. Concluding remarks

A non-linear theory for vibrations of shallow cables has been formulated. The basic assumptions are moderate sag and the absence of spatial variation of the cable force component along the chord. The latter assumption permits the axial components of the problem to be eliminated by integration as in the corresponding linear theory by Irvine [11].

In particular the response to harmonic transverse load has been investigated by expanding the solution in the damped modes of the corresponding linearized problem. Because of the shallow cable assumptions the non-linear part of the response can be reduced to the analysis of a 2 d.o.f. system, involving a single vertical and a single horizontal mode. It is demonstrated that both undamped and damped vibrations may bifurcate into a state of whirling motion, where vertical and horizontal motion of comparable amplitude takes place at a phase difference close to $\frac{1}{2}\pi$.

It is shown that a pair of independent dampers acting in the vertical and horizontal direction, respectively, can reduce in-plane as well as whirling motion if appropriately tuned. The study indicates that tuning of both dampers determined to the optimal values of the linearized theory provide effective damping, reducing the amplitudes as well as the resonant frequency range. Reduction of the whirling motion depends on near optimal tuning of both dampers.

Acknowledgements

This work has been supported by the Danish Technical Research Council through the project Damping Mechanisms in Dynamics of Structures and Materials.

References

[1] S.C. Watson, D. Stafford, Cables in trouble, Civil Engineering, American Society of Civil Engineers 58 (4) (1988) 38–41.
[2] I. Kovacs, Zur Frage der Seilschwingungen und der Seildampfung, Die Bautechnik 59 (10) (1981) 325–332.
[3] S. Krenk, Vibrations of a taut cable with an external damper, Journal of Applied Mechanics 67 (2000) 772–776.
[4] S. Krenk, S.R.K. Nielsen, Vibration of a shallow cable with a viscous damper, Proceedings of the Royal Society, London, A 458 (2001) 339–357.
[5] S.I. Al-Noury, S.A. Ali, Large amplitude vibrations of parabolic cables, Journal of Sound and Vibration 101 (1985) 451–462.
[6] G.V. Rao, R. Iyengar, Internal resonance and non-linear response of elastic cable under periodic excitation, Journal of Sound and Vibration 149 (1991) 25–41.
[7] S.R.K. Nielsen, P.H. Kirkegaard, Super and combinatorial harmonic response of flexible elastic cables with small sag, Journal of Sound and Vibration 251 (1) (1992) 79–102.
[8] N.C. Perkins, Modal interactions in the non-linear response of elastic cables under parametric/external excitation, International Journal of Non-Linear Mechanics 27 (1992) 233–250.
[9] C.L. Lee, N.C. Perkins, Non-linear oscillations of suspended cables containing two-to-one internal resonance, Non-Linear Dynamics 3 (1992) 465–490.
[10] C.L. Lee, N.C. Perkins, Three-dimensional oscillations of suspended cables involving simultaneous internal resonance, Proceedings of ASME Winter Annual Meeting, AMD-14, 59–67, 1992.
[11] H.M. Irvine, Cable Structures, Dover, New York, 1992.
[12] S. Krenk, Damping and complex modes in dynamic response of structural elements, Technical University of Denmark, in press.